



HAL
open science

GaAs photonic crystal cavity with ultrahigh Q: microwatt nonlinearity at $1.55\mu\text{m}$

Sylvain Combrié, Alfredo de Rossi, Quynh Vy Tran, Henri Benisty

► **To cite this version:**

Sylvain Combrié, Alfredo de Rossi, Quynh Vy Tran, Henri Benisty. GaAs photonic crystal cavity with ultrahigh Q: microwatt nonlinearity at $1.55\mu\text{m}$. *Optics Letters*, 2008, 33 (16), pp.1908. <hal-00573059>

HAL Id: hal-00573059

<https://hal.science/hal-00573059v1>

Submitted on 24 Aug 2022

HAL is a multi-disciplinary open access archive for the deposit and dissemination of scientific research documents, whether they are published or not. The documents may come from teaching and research institutions in France or abroad, or from public or private research centers.

L'archive ouverte pluridisciplinaire HAL, est destinée au dépôt et à la diffusion de documents scientifiques de niveau recherche, publiés ou non, émanant des établissements d'enseignement et de recherche français ou étrangers, des laboratoires publics ou privés.



Distributed under a Creative Commons CC BY-NC 4.0 - Attribution - Non-commercial use - International License

GaAs photonic crystal cavity with ultrahigh Q : microwatt nonlinearity at $1.55 \mu\text{m}$

Sylvain Combrié,^{1,*} Alfredo De Rossi,¹ Quynh Vy Tran,¹ and Henri Benisty²

¹Thales Research and Technology, route départementale 128, 91767 Palaiseau, France

²Laboratoire Charles Fabry, CNRS, Institut d'Optique Graduate School, 91127 Palaiseau, France

*Corresponding author: sylvain.combrie@thalesgroup.com

We have realized and measured a GaAs nanocavity in a slab photonic crystal based on the design by Kuramochi *et al.* [Appl. Phys. Lett. **88**, 041112 (2006)]. We measure a quality factor $Q=700,000$, which proves that ultrahigh Q nanocavities are also feasible in GaAs. We show that owing to larger two-photon absorption in GaAs nonlinearities appear at the microwatt level and will be more functional in gallium arsenide than in silicon nanocavities.

The achievement of quality factors of $Q \approx 10^6$ [1,2] in micrometer-sized nanocavities carved in two-dimensional photonic crystals (PhC) opens perspectives for all-optical signal processing. The unique property of PhC cavities is their ultrasmall volume (of the order of $0.1 \mu\text{m}^3$) which, combined with a high Q factor, dramatically enhances the light-matter interaction. This is highly desirable for fundamental investigations in cavity quantum electrodynamics (QED) in condensed matter, where a single emitter, e.g., a quantum dot (QD), is strongly coupled to a single optical mode. As emission linewidth of a single QD can be as small as a few microelectronvolts at low temperature [3], reaching a comparable linewidth for the cavity resonance is clearly desirable. Besides QED and applications to microlasers and nonconventional laser sources such as single photon emitters for quantum key distribution, the strong enhancement of the light-matter interaction is fundamental to miniaturize a broad class of devices such as optical sensors and optical modulators. Furthermore, high Q values are compatible with broadband operation when a so-called coupled-resonator-optical-waveguide-type waveguide is built from multiple identical cavities [4]. For slow-light purposes or for nonlinearity enhancement, the intrinsic Q factor determines the maximum amount of delay-enhancement that can be achieved. The state-of-the-art in high- Q PhC resonators has been achieved by NTT and Kyoto's teams [1,2] in silicon-based structures. There is a widespread consensus that silicon processing technology is superior to the III-V semiconductor and therefore there is little chance that PhCs based on III-V's approach the state-of-the-art. On the other hand, III-V's offer unique opportunities in photonics, in particular emission-amplification of light.

In this Letter, we show that GaAs can reach Q values similar to those of silicon, namely, $Q > 700,000$. This result opens new perspectives for realizations combining the features of III-V materials with the attractive properties of PhCs, including ultra-low-power nonlinear optics. Microwatt-level nonlinear operation can therefore be envisioned from the $\approx 5 \mu\text{W}$ threshold power value obtained in our previous re-

sults [5,6] for the lower quality factor $Q \approx 246,000$. With the linear bandwidth set at ≈ 1 GHz by the cavity, nonlinear processing of the microwatt optical signal in the 1 MHz–1 GHz window can be achieved. From the scaling laws of the various effects [Kerr, free-carrier plasma, two-photon absorption (TPA), thermo-optic], we pinpoint the more favorable capabilities of GaAs in this respect.

Our strategy was to consider the design that ensured the highest theoretical Q factor and that has also been implemented successfully in Si structures. At the time we designed the cavity, this was the design proposed in [1]. Our underlying idea is that this structure must also be the most robust against fabrication tolerances. Three-dimensional finite-difference time-domain (FDTD3D) modeling predicted a Q factor of about 100×10^6 . We used a 186-nm-thick GaAs membrane and a basic lattice pitch $a=420$ nm. As shown in Fig. 1(a), the access waveguide is designed as W1.07 (W1 refers to the single missing row waveguide along the ΓK direction of the photonic crystal), while the width of the structure supporting the cavity is Wx , with x variable but $x < 1$. The hole shifts defining the cavity are 9, 6, and 3 nm. The waveguide-cavity separation varies between 7 and 9 rows.

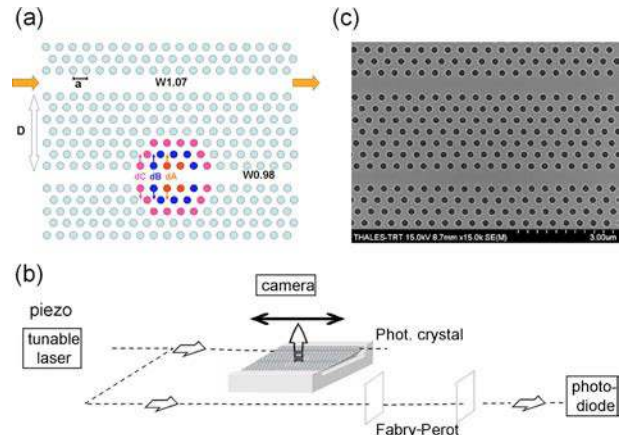


Fig. 1. (Color online) (a) Schematic of the GaAs side-coupled cavity system, (b) experimental setup, (c) SEM image of the cavity.

We used a compact and efficient 100 kV e -beam writer nB3 (NanoBeam Ltd., Cambridge, UK) to define the patterns in the top resist layer, the rest being unchanged. The good results obtained validate the qualities of this tool. Inductively coupled reactive-etching [7] was used to perform GaAs/GaInP vertical etching. As for measurements, we used a tunable laser source (Tunics from Nettek) operated in the fine scanning mode by applying an external voltage. The wavelength shift is monitored with a low-finesse Fabry–Perot (FP) interferometer [Fig. 1(b)] with 28.6 cm spaced mirrors (free-spectral range is 526 MHz). We have fabricated nine cavities with slightly modified parameters (controlling the coupling strength to the waveguide) and measured four of them (3, 4, 5, and 7). Cavities 5 and 7 have been designed for maximizing Q with purposely weak coupling ($x=0.98$ and spacing is 9 rows); the two other cavities (3 and 4) have nonoptimal parameters and were designed with a stronger waveguide to cavity coupling. Measurements have been performed at different power levels to identify the linear regime whereby the Q factor saturates as power is further reduced. Each of these measurements has been repeated ten times. The uncertainty is deduced from the fitting procedure and also corresponds to the fluctuation across measurements. Figure 2 shows the measurement for cavity 5. The signal detected from the top of the cavity provides a peak at resonance [Fig. 2(a)], while the transmitted waveguide signal displays a corresponding dip [Fig. 2(b)] whose depth is indicative of coupling conditions [6]. A largely sub-critical coupling was observed (the minimum-maximum transmission ratio at resonance being $T_m/T_M \approx 90\%$). The value for the loaded Q factor [Lorentzian fit, averaged over several measurements,

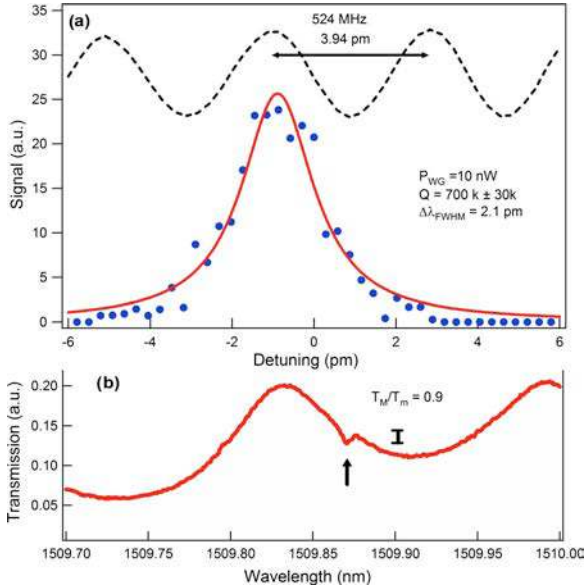


Fig. 2. (Color online) Spectra of the resonance of cavity 5. The power coupled into the waveguide is about 10 nW. (a) Detected signal from the camera as a function of the detuning (markers) and Lorentzian fit (solid curve). Transmission of the FP interferometer used as reference (dashed curve). (b) Transmitted signal through the waveguide. The cavity resonance is pointed out by the arrow.

Fig. 2(a)] was $Q=700,000 \pm 30,000$ ($\Delta\nu=280$ MHz, $\Delta\lambda=2.1$ pm). The estimated optical power coupled into the waveguide is here about 10 nW. The fraction of power P_c/P_{wg} actually coupled into the cavity is $P_c/P_{wg}=2(\sqrt{T_m/T_M}-T_m/T_M) \approx 0.1$, which makes 1 nW. We had to stick to such small values to prevent broadening induced by nonlinear absorption. We have also measured $Q \approx 700,000$ in cavity 7. In spite of the progress made in PhC microcavities, the gap between theoretical expectation and experimental measurements of the Q factor is large: Here it is almost 2 order of magnitude. This holds also for silicon. This suggests that the limit of processing capability is close, even for state-of-the-art e -beam systems. The important point of this work is that the handicap of III–V processing with respect to silicon has almost vanished. We are convinced that the residual gap separating us from the world record is rather related to residual structural disorder (e -beam lithography and plasma etching). We think that other factors, such as residual absorption in the material, are still negligible in this spectral range. We also believe that our process (high-density plasma) generates a relatively low number of surface defects so that an additional source of losses is avoided.

A Q scaling from our previous work [5] indicates that for such high values of the Q factor we enter into a nonlinear regime at the microwatt level in terms of power flow in the waveguide. This is confirmed in Fig. 3, where we report the dependence of the line shape of another cavity than that of Fig. 2 as a function of the power coupled in the waveguide. The onset of nonlinearity (here T Photon A) appears as the power coupled to the waveguide is of the order of $0.3 \mu\text{W}$.

However, as underlined by both this and previous work [8], both thermal and electronic nonlinearities are involved: Kerr effect, TPA, and the resulting index changes due to free-carrier plasma and the thermo-optic effect. For thermo-optic effects, at first sight, silicon is a better heat conductor. We show be-

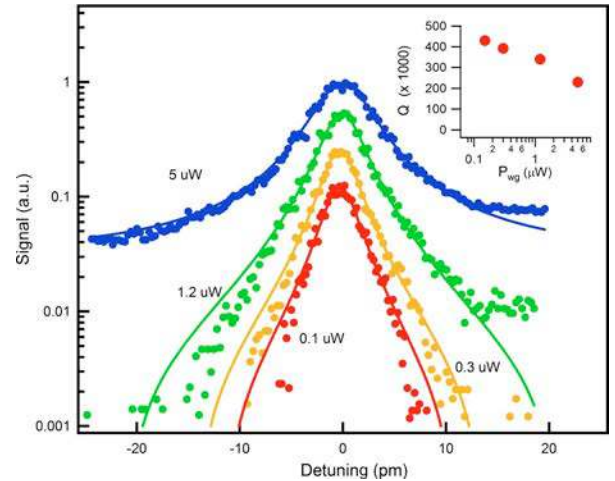


Fig. 3. (Color online) Cavity 3. Signal detected from the cavity (log scale) as a function of the detuning at different optical powers coupled in the waveguide (P_{wg}). The curves are shifted vertically for clarity. Inset, dependence of the Q factor on P_{wg} .

low that this appearance is largely offset by the intrinsic lower operation point of GaAs, giving to this latter material a clear niche for ultra-low-power optical manipulations. Let us detail how the nonlinear operation can be performed to further evaluate GaAs versus Si. First, in transient operation the thermo-optic effect has a time-dependent spatial extent x , given by the thermal diffusivity C_p , obeying the $x \approx (C_p \tau)^{1/2}$ scaling (where C_p is 0.31 and 0.78 m²/s for GaAs and Si, respectively). In the megahertz to gigahertz range x is submicrometric, and the heat resulting from TPA will still reside within the cavity, not even spreading beyond one PhC lattice pitch [9]. This implies the virtual impossibility to implement an extra thermal sink at these high Q -low nonlinear threshold values. Second, the TPA damping threshold (at which the induced damping halves Q) is evaluated in terms of power coupled through the cavity P_c as $P_c^{\text{th}} = (4\pi^2 V_{\text{TPA}}) / (\lambda^2 Q^2 \beta) \propto \beta^{-1}$. Here the TPA constant is $\beta = 10$ cm/GW for GaAs and the nonlinear effective volume is about 0.4 μm^3 . This amounts to approximately 100 nW for a mean quality factor $Q = 7 \times 10^5$. This is in quite good agreement with data measured on cavity 3 in Fig. 3 where the estimated power at which the Q factor drops is $P_{\text{WG}}^{\text{th}} \approx 2 \mu\text{W}$ in the waveguide and therefore much lower in the cavity, due to the weak coupling. We have also measured the power for cavity 5 and found that Q drops to 500,000 as power in the waveguide is raised to 1 μW , i.e., 100 nW in the cavity. Third, the impact of thermo-optic effects derives from the index shift Δn , which is proportional to the thermo-optical coefficient n_T , the thermal resistance, and the amount of power absorbed, which turns out to be governed by the ratio $n_T / (\beta C_p)$. This is a key point: Obviously, a stronger TPA coefficient and a lower power threshold weakens the thermal burden. Of particular interest here is the fact that the ≈ 4 times weaker n_T / C_p ratio of silicon is well offset by the > 10 times larger TPA coefficient β of GaAs.

Fourth, the carriers generated by TPA induce a negative index shift counteracting the Kerr effect. This is governed by the carrier recombination time τ_{rec} , which can be considered to be fast (τ_{rec} is in the 10–100 ps time scale [8,10]). The amount of energy stored in the cavity W at which the plasma-induced index change takes over the Kerr effect is $W_{\text{th}} \approx n_2 m^* / (\beta \tau_{\text{rec}})$, with m^* being the effective electron mass and n_2 being the Kerr coefficient. With the values 1.6 and 0.45 cm²/GW for n_2 in GaAs and Si, respectively, the crossover energy ratio is $W_{\text{th,Si}} / W_{\text{th,GaAs}} \approx 15 \times \tau_{\text{rec,GaAs}} / \tau_{\text{rec,Si}}$. Moreover, the net

ratio is almost entirely compensated when considering typical values for τ_{rec} : 100 ps for Si and 10 ps for GaAs [10], resulting in similar crossover powers. Usually, the Kerr effect is sought for optical manipulation and TPA is seen as an hindrance. Taking an opposite approach, i.e., exploiting nonlinear cavity damping, it becomes advantageous to use GaAs: As it operates at a much lower power, it features less index shift from the Kerr effect than silicon.

In conclusion, we showed that an ultrahigh Q nanocavity akin to those elaborated in silicon is also feasible in GaAs, making GaAs devices with $Q \approx 10^6$ fully plausible. Additionally, we stressed the possibility to operate at the microwatt level for nonlinear operation, through nonlinear damping based on two-photon-absorption. Importantly, we substantiated the fact that thermal effects inflict less severe penalties when operating nanocavities based on GaAs as compared to those based on Si.

We acknowledge the support of the SESAME action of Conseil Général Ile de France for key equipment used in this work. S. Combrié, A. De Rossi, and Q. V. Tran acknowledge the financial support of the European Commission through the IST Project “QPhoton.”

References

1. E. Kuramochi, M. Notomi, S. Mitsugi, A. Shinya, and T. Tanabe, *Appl. Phys. Lett.* **88**, 041112 (2006).
2. S. Noda, M. Fujita, and T. Asano, *Nat. Photonics* **1**, 449 (2007).
3. A. Berthelot, I. Favero, G. Cassabois, C. Voisin, C. Delalande, Ph. Roussignol, R. Ferreira, and J. M. Gérard, *Nat. Phys.* **2**, 759 (2006).
4. T. Tanabe, M. Notomi, E. Kuramochi, A. Shinya, and H. Taniyama, *Nat. Photonics* **1**, 49 (2007).
5. E. Weidner, S. Combrié, A. De Rossi, Q.-V. Tran, and S. Cassette, *Appl. Phys. Lett.* **90**, 101118 (2007).
6. S. Combrié, E. Weidner, A. De Rossi, S. Bansropun, S. Cassette, A. Talneau, and H. Benisty, *Opt. Express* **14**, 7353 (2006).
7. S. Combrié, S. Bansropun, M. Lecomte, O. Parillaud, S. Cassette, H. Benisty, and J. Nagle, *J. Vac. Sci. Technol. B* **23**, 1521 (2005).
8. T. Uesugi, B. S. Song, T. Asano, and S. Noda, *Opt. Express* **14**, 377 (2006).
9. A. De Rossi, M. Lauritano, S. Combrié, Q.-V. Tran, and C. Husko, “Interplay of plasma-induced and fast thermal nonlinearities in a GaAs-based photonic crystal nanocavity” (submitted to *Phys. Rev. A*).
10. A. D. Bristow, J.-P. R. Wells, W. H. Fan, A. M. Fox, M. S. Skolnick, D. M. Whittaker, A. Tahraoui, T. F. Krauss, and J. S. Roberts, *Appl. Phys. Lett.* **83**, 851 (2003).